Archives of Biochemistry and Biophysics 584 (2015) 79–89

Contents lists available at ScienceDirect

Archives of Biochemistry and Biophysics

journal homepage: www.elsevier.com/locate/yabbi

Proteoliposomes with the ability to transport Ca^{2+} into the vesicles and hydrolyze phosphosubstrates on their surface

Maytê Bolean [a], Ana Maria S. Simão [a], Tina Kiffer-Moreira [b], Marc F. Hoylaerts [c], José Luis Millán [b], Rosangela Itri [d], Pietro Ciancaglini [a, *]

[a] Depto. Química, FFCLRP-USP, Universidade de São Paulo, Ribeirão Preto, SP, Brazil
[b] Sanford Children's Health Research Center, Sanford Burnham Prebys Medical Discovery Institute, La Jolla, CA, USA
[c] Department of Cardiovascular Sciences, Center for Molecular and Vascular Biology, University of Leuven, Leuven, Belgium
[d] Depto. Física Aplicada, Instituto de Física, IF-USP, São Paulo, SP, Brazil

ARTICLE INFO

Article history:
Received 26 March 2015
Received in revised form
26 August 2015
Accepted 27 August 2015
Available online 29 August 2015

Keywords:
Annexin V
Alkaline phosphatase
Matrix vesicles
DPPC
DPPS
Liposome
Calorimetry
Proteoliposome

ABSTRACT

We describe the production of stable DPPC and DPPC:DPPS-proteoliposomes harboring annexin V (AnxA5) and tissue-nonspecific alkaline phosphatase (TNAP) and their use to investigate whether the presence of AnxA5 impacts the kinetic parameters for hydrolysis of TNAP substrates at physiological pH. The best catalytic efficiency was achieved in DPPS 10%-proteoliposomes (molar ratio), conditions that also increased the specificity of TNAP hydrolysis of PP_i. Melting behavior of liposomes and proteoliposomes was analyzed via differential scanning calorimetry. The presence of 10% DPPS in DPPC-liposomes causes a broadening of the transition peaks, with AnxA5 and TNAP promoting a decrease in ΔH values. AnxA5 was able to mediate Ca^{2+}-influx into the DPPC and DPPC:DPPS 10%-vesicles at physiological Ca^{2+} concentrations (~2 mM). This process was not affected by the presence of TNAP in the proteoliposomes. However, AnxA5 significantly affects the hydrolysis of TNAP substrates. Studies with GUVs confirmed the functional reconstitution of AnxA5 in the mimetic systems.

These proteoliposomes are useful as mimetics of mineralizing cell-derived matrix vesicles, known to be responsible for the initiation of endochondral ossification, as they successfully transport Ca^{2+} and possess the ability to hydrolyze phosphosubstrates in the lipid–water interface.

1. Introduction

Endochondral calcification is mediated by chondroblast- and osteoblast-derived matrix vesicles (MVs). Chondrocytes and osteoblasts control the composition of the extracellular matrix and also release MVs (structures ranging from 100 to 300 nm in diameter), considered by some to serve as the initial sites of hydroxyapatite (HA) mineral formation [1–7] where the deposition of seed mineral (nucleation) takes place [8–10]. Ion channels and transporters present in MV membranes are responsible for the uptake of diverse ions into these organelles [8] and promote intraluminal crystal growth [11].

Two protein families present in MVs merit special attention: annexins and phosphatases. The annexins constitute a large family of acidic phospholipid-dependent Ca^{2+}-binding proteins that play a major role in the initiation of mineralization by MVs [11,12]. Twelve different annexins have been isolated from a large variety of cell types and proteomic assays showing that annexins are the most abundant proteins detected in MVs [9]. Human Annexin V (AnxA5), a protein of ~33 kDa, was the first to be characterized by crystallography [13,14], revealing a slightly curved molecule in which each of the four repeats fold into a compact domain consisting of five α-helices [14]. These domains are arranged to define a hydrophilic pore through the center of the protein. Such a pore presents Ca^{2+}-channel activity in the MV membrane [9,11,15]. AnxA5 is also responsible for other physiological events, such as phospholipid-dependent inhibition of blood coagulation [16,17], modulation of protein kinase C [18], inhibition of phospholipase A2 activity [19] and cellular disorganization resulting in apoptosis process [9,15]. The expression of annexins is up-regulated in mineralization-competent tissue, and these annexins are relocated to the plasma membrane followed by the release of annexin-containing MV. Recent studies have implicated at least three phosphatases in the

* Corresponding author. Depto Química, FFCLRP-USP, Av. Bandeirantes, 3900, 14040-901 Ribeirão Preto, SP, Brazil. Tel.: +55 1633153753; fax: +55 1633154838.
E-mail address: pietro@ffclrp.usp.br (P. Ciancaglini).

http://dx.doi.org/10.1016/j.abb.2015.08.018
0003-9861/

initiation of skeletal mineralization, Tissue non-specific alkaline phosphatase (TNAP), PHOSPHO1 and ENPP1 [20,21]. TNAP is a glycosylphosphatidylinositol (GPI)-anchored membrane ectoenzyme [22–24] in contact with extracellular cartilage fluid, where natural substrates (adenosine 5′-triphosphate (ATP), adenosine 5′-diphosphate (ADP), inorganic pyrophosphate (PP_i)) are present at nanomolar or micromolar concentrations [25]. The GPI anchor structure results in mobility of the enzyme on biological membranes [25–27].

We have previously demonstrated that the presence of charged lipids [25] and cholesterol [7] in the mimetic systems, or proteoliposomes with more complex lipid composition [28] can affect the catalytic properties of the anchored TNAP. In particular, TNAP is well incorporated in 1,2-dipalmitoyl-sn-glycero-3-phosphocholine (DPPC)-liposomes at 25 °C. Interestingly, TNAP-containing proteoliposomes constituted by DPPC, which is in a gel phase at this temperature, are more stable over time than others composed by unsaturated lipids, which are in a fluid phase at the same temperature [7,26,28].

Noteworthy, it is known that GPI-anchored proteins like TNAP are preferentially located in the ordered lipid phase region of the cell plasma membrane [29]. In fact, previous reports evidenced that GPI-anchored intestinal alkaline phosphatase is spontaneously inserted in DPPC-enriched gel phase [29]. The primary function of TNAP is related to degradation of extracellular PP_i (ePP_i), a mineralization inhibitor produced by nucleotide pyrophosphatase/phosphodiesterase-1 (ENPP1), thus controlling ePP_i concentrations to maintain a P_i/PP_i ratio permissive for normal bone mineralization [7,25–30].

In addition, several studies have demonstrated that TNAP hydrolyzes ATP, releasing P_i. The enzyme is regulated by the ATP concentration [31] and inhibited by the product of the reaction (P_i) [32], suggesting that the relative levels of PP_i and P_i present in the extracellular matrix play a role in the regulation of the mineralization process. It has been demonstrated that TNAP generates PP_i through its phosphodiesterase activity, hydrolyzing ATP [33], although one of its primary functions is to remove PP_i from the mineralization microenvironment through its phosphomonohydrolase activity [8,10,34–36].

Acid phospholipids, especially phosphatidylserine, which have great affinity for calcium, are usually found in the membrane of MVs [37], being able to promote hydroxyapatite formation *in vitro*, even in the absence of TNAP [38]. These studies suggest a possible association of phospholipids with the mineralization process.

Some authors suggest that lipids are involved in bone formation. For example, phospholipids can facilitate cartilage mineralization in the growth plate [6,9]. DPPC and 1,2-dipalmitoyl-sn-glycero-3-phospho-L-serine (DPPS) are two of the main lipids found in MV membranes [4–6,9], and many studies have revealed that they play a crucial role in the biomineralization process, regulating both the calcium entry into the MVs and the formation of hydroxyapatite crystals [9,15,39–41]. The MVs membrane containing phosphatidylserine-rich domains may offer an ideal environment for optimal protein–protein and protein-lipid interactions and optimal function of AnxA5 in Ca^{2+} influx and cartilage matrix mineralization [15].

In the present study, we standardized the preparation of proteoliposomes composed of DPPC and DPPC:DPPS (at different molar ratios), which harbor TNAP and AnxA5 concomitantly, with the aim of mimicking MVs. We characterized the thermal behavior of these proteoliposomes by means of differential scanning calorimetry (DSC) as well as their stability by dye-leakage assays and dynamic light scattering measurements (DLS). Enzymatic activity, calcium uptake measurements and phase contrast microscopy of giant proteoliposomes demonstrated the functional incorporation of both proteins. This is an intermediate system with two main proteins that will give support to the design and construction of more complex MVs mimetic systems.

2. Materials and methods

2.1. Materials

All aqueous solutions were made using Millipore DirectQ ultra pure apyrogenic water. Bovine serum albumin (BSA), tris hydroxymethyl-amino-methane (Tris), ATP, ADP, PP_i, sodium dodecylsulfate (SDS), dexamethasone, glucose 1-phosphate, glucose 6-phosphate, fructose 6-phosphate, β-glycerophosphate, polyoxyethylene-9-lauryl ether (polidocanol), α-naphthyl phosphate, Fast Blue RR, 2′,7′bis(carboxymethyl)-aminomethylfluorescein (CF), sucrose, glucose, HCl, $MgCl_2$, NaOH, NaCl, $CaCl_2$, KCl, $NaHCO_3$, KH_2PO_4, ethylene glycol-bis(2-aminoethylether)-N,N,N′,N′-tetraacetic acid (EGTA), were from Sigma Chemical Co. (St Louis, MO, USA), Calbiosorb resin (Merck Chemicals), 1,2-dipalmitoyl-sn-glycero-3-phosphocholine (DPPC), 1,2-dipalmitoyl-sn-glycero-3-phospho-L-serine (DPPS) and 1,2-dioleoyl-sn-glycero-3-phosphocholine (DOPC) were from Avanti Polar Lipids, Inc., $^{45}CaCl_2$ (PerkinElmer, Inc.), Amicon Ultra 30 K device (30,000 NMWL), 75 cm^2 plastic culture flasks were from Corning (Cambridge, MA, USA). α-MEM, fetal bovine serum, ascorbic acid, gentamicin and fungizone were from Gibco-Life Technologies (Grand Island, NY, USA). Analytical grade reagents were used without further purification.

2.2. Expression of AnxA5

The plasmid for AnxA5 (pProEx.Htb.annexin V) was kindly provided by Prof. Seamus J. Martin from Dublin (Ireland). Human AnxA5 cDNA (accession no. NM_001154) was amplified from a Jurkat cDNA library through PCR and cloned into the bacterial expression vector pProEx.Htb using the restriction sites BamHI and EcoRI. The pProEx.Htb vector contains an ampicillin resistance cassette and encodes an N-terminal poly-histidine tag to facilitate purification of proteins expressed with this epitope tag. The ampicillin resistance gene enables selection and growth of colonies expressing the pProEx.Htb.annexin V plasmid. The Trc promoter within the pProEx.Htb.annexin V plasmid is under the control of the lacI repressor and can be activated by the addition of isopropyl-b-Dthiogalactopyranoside (IPTG) (a lactose analog) to the bacterial growth medium, thereby inducing expression of recombinant AnxA5 protein with an N-terminal poly-histidine tag. Polyhistidine – tagged proteins bind with high affinity to nickel or cobalt ions. Ni–nitrilotriacetic acid (NTA) agarose can then be used to capture and purify the recombinant AnxA5 from bacterial lysates [42].

2.3. Rat bone marrow cell isolation, culture and preparation of membrane-bound alkaline phosphatase

Cells were prepared and cultured according to Simão et al. [43]. Membrane-bound alkaline phosphatase, an osteoblast-specific marker, was prepared from cell culture as described by Simão et al. [24,43]. Protein concentrations were estimated according to Hartree [44] in the presence of 2% (w/v) SDS. BSA was used as standard.

2.4. Enzymatic activity measurements

p-Nitrophenylphosphatase (p-NPPase) activity was assayed discontinuously at 37 °C as previously described [24,43]. The reaction was initiated by the addition of the enzyme and stopped

with 0.5 mL of 1 mol/L NaOH at appropriate time intervals [26]. For ATP, ADP and PPi hydrolysis, the phosphomonohydrolase activities were assayed discontinuously by measuring the amount of inorganic phosphate liberated as before [23], adjusting the assay medium to a final volume of 0.5 mL. All determinations were carried out in duplicate and initial velocities were constant for at least 90 min, provided that less than 5% of substrate was hydrolyzed. Controls without added enzyme were included in each experiment to correct for non-enzymatic hydrolysis of substrate. One enzyme unit (1 Unit) was defined as the amount of enzyme hydrolyzing 1.0 nmol of substrate per min at 37 °C per mg of protein. Maximum velocity (V_M), apparent dissociation constant ($K_{0.5}$), and Hill coefficient (n) obtained from substrate hydrolysis were calculated as described [45]. Data were reported as the mean ± S.D. of triplicate measurements of 3 different enzyme preparations. Statistical comparisons were accomplished by two-way ANOVA followed by Bonferroni's test all data sets. P values ≤ 0.05 are considered significant.

2.5. Solubilization of TNAP with polidocanol

Membrane-bound TNAP (0.02 mg/mL of total protein) was solubilized with 1% polidocanol (w/v) (final concentration) as described by Ciancaglini et al. [46]. Detergent removal was performed as described by Camolezi et al. [26] and Simão et al. [47].

2.6. Liposome preparation

The lipids DPPC and DPPS were used in the preparation of the DPPC liposomes and DPPC:DPPS liposomes with 5, 10 and 15% of DPPS (molar ratio). Lipids were dissolved in chloroform and dried under nitrogen flow. The resulting lipid film was kept under vacuum overnight and suspended in 50 mmol/L Tris–HCl buffer, pH 7.5, containing 2 mmol/L $MgCl_2$ and 200 μM EGTA, obtaining a final solution of 1.5 mg/mL (DPPC:DPPS). The mixture was then incubated for 1 h at 70 °C, above the critical phase transition temperature of the lipid, and vortexed at 10 min intervals. Large unilamellar vesicles (LUVs) were prepared by submitting the suspension to extrusion through 100 nm polycarbonate membranes in a LiposoFast extrusion system (Liposofast, Sigma–Aldrich). LUVs were prepared and used in the same day as described by Bolean et al. [7,28].

2.7. Incorporation of TNAP into liposomes

Proteoliposome was prepared by direct insertion method using equal volumes of liposomes (1.5 mg/mL) and TNAP (0.02 mg/mL) resulting in a 1:15,000 protein:lipid ratio, as previously described by Bolean et al. [7,28] and Simão et al. [47]. TNAP activity of the supernatant and the resuspended pellet was assayed and used to calculate the percent of protein incorporation [47].

2.8. Incorporation of TNAP and AnxA5 into liposomes

TNAP (0.02 mg/mL) and AnxA5 (0.2 mg/mL) were incorporated into DPPC and DPPC:DPPS liposomes (5–15% DPPS molar ratio) by direct insertion in 50 mM Tris–HCl buffer, pH 7.5, containing 2 mM $MgCl_2$ and 200 μM EGTA, resulting in a 1:15,000 and 1:100 (protein:lipid ratio) respectively. The mixture was incubated overnight at 25 °C to avoid possible thermal inactivation. Then, the mixture was ultracentrifuged at 100,000 × g during 1 h, at 4 °C. The pellet containing proteoliposomes was resuspended in the initial volume of the same buffer. The p-NPPase activity present in both pellet and supernatant was used to determine the percentage of incorporation into the liposome [47]. All proteoliposomes were prepared and used immediately or stored at 4 °C for a maximum of two days.

To quantify the amount of each of the proteins in the proteoliposomes, we chose to work with DPPC and DPPC:DPPS 10%-vesicles (molar ratio) and treated them with phosphatidylinositol-specific phospholipase C (PIPLC), as described by Pizauro et al. [23]. After ultracentrifugation, both proteins concentrations were analyzed in the supernatant (TNAP) and pellet (AnxA5).

Controls to study membrane-damaging activity were evaluated, at 37 °C, by the release of a self-quenched fluorescent dye (25 mM CF) entrapped in the aqueous pool of either liposome or proteoliposome. Changes of membrane permeability due to lipid bilayer disruption, membrane defects or pores formation leads to a dilution of CF to the external membrane solution resulting in an increase of the fluorescence signal [48,49].

2.9. Dynamic light scattering measurements (DLS)

The determination of liposomes and proteoliposomes size distribution was performed by dynamic light scattering, using a N5 Submicron Particle Size Analyzer (Beckman Coulter, Inc., Fullerton, CA, USA). Average value (n = 5) of the liposomes diameters was obtained at 25 °C by unimodal distribution, previously filtered (0.8 μm) [7,28].

DLS measurements for liposomes and proteoliposomes were performed throughout the period of use of the samples (7 days) and both diameter and intensity varied less than 5%, when stored at 4 °C.

2.10. Differential scanning calorimetry (DSC)

Transition phase temperatures (T_m) of the LUVs membranes prepared with different lipid compositions were studied by DSC. All LUVs suspensions and reference buffer employed in the experiment were previously degasified under vacuum (140 mbar) for 30 min.

The samples and reference (buffer) were scanned from 10 °C to 90 °C at an average heating rate of 0.5 °C/min, under pressure of 3 atm and the recorded thermograms were analyzed using a Nano-DSC II – Calorimetry Sciences Corporation, CSC (Lindon, Utah, USA). The baseline was determined by filling the sample and the reference cells with buffer solution. Data was analyzed with the fitting program CpCalc provided by CSC. The thermograms shown in the figures correspond to the first scan, but at least three heating and cooling scans were performed for each analysis [7,28].

2.11. Calcium uptake by liposomes and proteoliposomes systems

The calcium uptake was assessed using an adaptation of a protocol reported by Hsu and Camacho [50]. Briefly, aliquots of proteoliposomes harboring AnxA5 or TNAP + AnxA5, with different compositions (DPPC or DPPC:DPPS 10%), and protein-free liposomes were incubated at 37 °C in a reaction media (1:1 v/v) for 19 h. The reaction media consisted of 50 mM Tris, pH 7.65, 85 mM NaCl, 15 mM KCl, 1 mM $MgCl_2$, 30 mM $NaHCO_3$ and 2.3 mM KH_2PO_4; $^{45}Ca^{2+}$ (5.5 μCi/mL) was used as a tracer. Curves of the calcium cold concentration were done from 0.5 to 5 mM $CaCl_2$. Samples were filtered through Amicon Ultra 30 K device (30,000 NMWL) and after washing the radioactivity associated to inner compartment of the proteoliposomes was determined by scintillation counting. The background $^{45}Ca^{2+}$ uptake was defined as the radioactivity bound to the filters under identical conditions in the presence of vesicles without proteins (liposomes) with the same lipid compositions employed for the proteoliposomes (DPPC-liposomes or DPPC:DPPS 10%-liposomes).

2.12. Incorporation of AnxA5 into giant unilamellar vesicles (GUVs)

2.12.1. GUVs preparation

GUVs were prepared by the electroformation procedure [51] and were composed of pure DOPC and DOPC:DPPS 10% (molar ratio): 20 μl of 2 mg/ml lipid chloroform solution of desired composition was spread on the surfaces of two conductive glass slides coated with indium tin oxide. The glass slides were placed with their conductive sides facing each other and separated by a 2 mm thick Teflon® frame. The chamber was filled with 0.2 M sucrose solution containing 0.5 mM $CaCl_2$ (see below) and placed inside an oven at ~55 °C. The glass plates were connected to a function generator and an alternating electric field of 2 V with a 10 Hz frequency was applied for 2 h. The vesicle solution was removed from the chamber and diluted ~10 times into a 0.2 M glucose solution. The osmolarities of the sucrose and glucose solutions were measured with a cryoscopic osmometer Osmomat 030 (Gonotec, Germany). Vesicles dispersed in glucose solution containing AnxA5 (8.22 μM) were immediately observed under the optical microscopy (see below). All measurements were done at room temperature (22–25 °C).

2.12.2. Optical microscopy observation and electro deformation procedure

Vesicles were observed in the phase contrast mode by means of an inverted microscope Axiovert 200 (Carl Zeiss; Jena, Germany) equipped with a Plan Neo-Fluar 63 × Ph2 objective (NA 0.75). Images were recorded with an AxioCam HSm digital camera (Carl Zeiss).

Electro deformation experiments were performed by submitting the samples to an alternating electric field (AC) of 10 V intensity and 1 MHz frequency [52–54]. Vesicles grown in the sucrose solution containing a small amount of salt (0.5 mM $CaCl_2$) ensure a higher conductivity in the inner compartment of the vesicle in respect to the outer solution that contains AnxA5 dispersed in glucose solution. The GUVs were then placed into a special chamber purchased from Eppendorf (Hamburg, Germany), which consists of 8 mm thick Teflon frame confined between two glass plates through which observation was possible. A pair of parallel platinum electrode wires with 90 μm in radius was fixed to the lower glass. The gap distance between the two wires was 0.5 mm. The chamber was branched to a function generator and the vesicles lying between the two parallel wires were observed.

3. Results and discussion

3.1. Proteoliposomes harboring TNAP and/or AnxA5

Previous studies by our group [7,26,28,47] reported a significant amount of TNAP activity incorporation into DPPC-liposomes (~95%) at 25 °C. At this temperature DPPC is in the gel phase ($T_m = 41.5$ °C), facilitating a good yield of enzyme insertion into the lipid systems [7,26,28]. As reported, the lipid microenvironment affects the insertion and activity of the enzyme [7,28,47].

Kirsch et al. [15] demonstrated the importance of DPPS for the efficient reconstitution of AnxA5 into vesicular systems. They reported that AnxA5 inserted spontaneously into liposomes containing different phosphatidylserine (PS) concentrations but not in liposomes constituted of phosphocholine (PC) or phosphatidylethanolamine (PE) only, probably due to the specific conditions applied (200 nM AnxA5 incubated with liposomes during 1 h at room temperature), which differ from our conditions (6 μM AnxA5 incubated with liposomes during 24 h at room temperature).

In order to obtain proteoliposomes harboring both proteins, DPPC:DPPS-containing lipid bilayers were initially tested for TNAP incorporation, at different molar ratios, starting with low DPPS concentrations (5–30% of DPPS in DPPC-liposomes) up to DPPC:DPPS 1:1 (molar ratio). As shown in Fig. 1, liposomes containing 5–15% of DPPS do not favor TNAP incorporation. On the other hand, DPPC:DPPS lipid bilayers composed of 20–30% of DPPS favor TNAP insertion, presenting similar incorporation percentages as that determined for pure DPPC of *circa* 40%. Remarkably, TNAP does not incorporate into DPPC:DPPS 1:1 (molar ratio) liposomes (<5%).

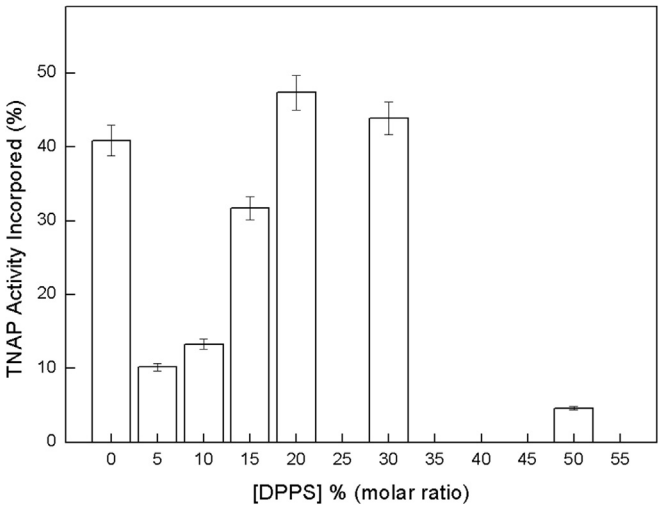

Fig. 1. Effect of increasing DPPS concentration into DPPC-liposomes on TNAP activity incorporation.

We thus focused on the standardization and characterization of proteoliposomes containing both proteins. Since in MVs, PS can represent of 9.3% [9] to 16.3% [4] of the total lipid composition we chose a maximum of 15% DPPS for liposome preparation.

As shown in Table 1, the presence of AnxA5 favors the incorporation of TNAP activity in DPPC liposomes. Similar behavior was observed when DPPS was present in the proteoliposome composition in the concentration range of 5–15%. This effect was more pronounced for proteoliposomes constituted of DPPC:DPPS 5% (molar ratio), where the presence of AnxA5 increased 6.4 fold the incorporation of TNAP activity, decreasing gradually for increasing concentrations of DPPS.

To quantify the amount of each protein incorporated into the proteoliposomes, we thus chose to construct DPPC and DPPC:DPPS 10%-vesicles (molar ratio) and then treated them with PIPLC [23] to recover after ultracentrifugation, TNAP in the supernatant and AnxA5 in the pellet. The protein quantifications revealed that TNAP and Anx5 represented 25% and 75%, respectively, of the total

Table 1
Percentage of phosphomonohydrolase activity by TNAP reconstituted in liposomes of different lipid compositions, in the absence and presence of AnxA5. TNAP activity was determined as described in Material and Methods using pNPP as substrate.

Proteoliposome composition			TNAP activity incorporated (%)	Relative improvement (fold)
Lipid (molar ratio)	TNAP	AnxA5		
DPPC 100%	+	–	40.9 ± 2.8	
	+	+	63.7 ± 4.5	1.6
DPPC:DPPS 5%	+	–	10.2 ± 2.3	
	+	+	65.1 ± 3.2	6.4
DPPC:DPPS 10%	+	–	19.3 ± 1.5	
	+	+	41.2 ± 3.6	2.1
DPPC:DPPS 15%	+	–	31.7 ± 2.9	
	+	+	48.9 ± 4.7	1.5

protein incorporated into the proteoliposomes, regardless DPPS presence.

Therefore, one can observe that AnxA5 affects the amount and the activity behavior of TNAP (Table 1). This effect will be better explored later on in the text.

Studies related to only AnxA5 incorporation show that this protein was able to incorporate into DPPC-proteoliposomes (11.6 ± 1.5 μg/mL), but the presence of DPPS increased significantly (>twice) the AnxA5 incorporation (25.8 ± 4.4 μg/mL). Therefore, although significant binding of AnxA5 into PC-based liposomes has previously not been reported [11,15], we could achieve AnxA5 incorporation into DPPC-liposomes, probably because our methodology employed a large amount of AnxA5 in solution, thus enabling its insertion into the DPPC lipid bilayer.

No release of fluorescent dye CF encapsulated in the proteoliposomes constituted by different lipid mixtures was observed during at least 2 days, at 37 °C. The release of dye is instantaneous following the addition of detergent. This strongly suggests the presence of unilamellar systems, which immediately disrupt after addition of the solubilizing agent (results not shown). It is also important to note that we have previously studied the reconstitution of TNAP [7,25–28] in liposomes with different defined lipid compositions. As observed from the results, the percentage of activity recovery of the phosphomonohydrolase activity reconstituted in PC-based liposomes increases with the increase of fatty acyl chain length, achieving maximum values of reconstitution with 16-carbon-long PC, probably due to the length of the GPI anchor [26].

Under our experimental conditions, DPPC and DPPC:DPPS proteoliposomes harboring TNAP and AnxA5 are not spontaneously leaky.

3.2. Kinetic studies

In order to investigate the effect of the liposome composition on the activity of the reconstituted TNAP, and especially to assess how the presence of AnxA5 and of negative charges from DPPS influences the enzyme activity, the kinetic parameters from the hydrolysis of known major TNAP substrates (ATP, ADP and PP_i) were determined (Table 2).

For DPPC-liposomes harboring TNAP alone, higher V_{max} values were observed for ATP and PP_i hydrolysis (Fig. 2). Higher and lower catalytic affinities ($K_{0.5}$) were observed for PP_i and ADP, respectively, when compared to ATP. Cooperative effects (n) were not observed for ATP hydrolysis, while positive and negative cooperativity was found for ADP and PP_i hydrolysis, respectively (Table 2).

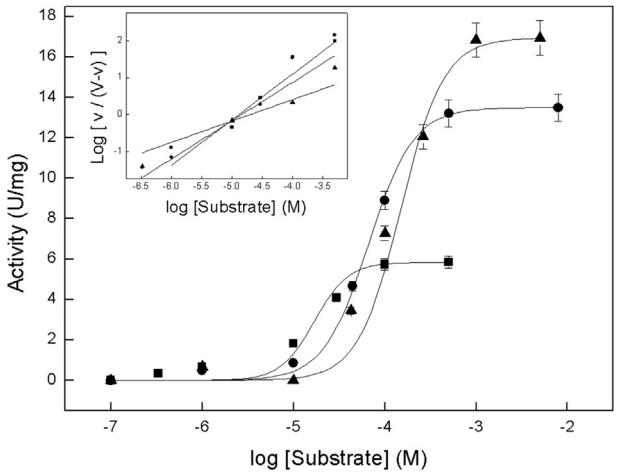

Fig. 2. Effect of increasing concentrations of (●) ATP, (■) ADP and (▲) PP_i substrates on the Pi-generating activity of DPPC-proteoliposomes harboring TNAP. Assays were done at 37 °C, buffered with 50 mM Tris–HCl, pH 7.4, containing 2 mM $MgCl_2$, and the P_i released was measured. Inset: Hill coefficient (n).

Both the modulation of the enzyme activity and insertion into the lipid microenvironment seem to be common between enzymes that have a GPI anchor [7,28,47,55]. The presence of positive charges (dioctadecyldimethylammonium bromide, DODAB), negative charges (DPPS) [47] and cholesterol-enriched ordered microenvironments [55] play a crucial role in the interaction between proteins and lipids [56–58] and, consequently, with biological membranes. Alkaline phosphatase from bovine intestine interacts in different ways with monolayers constituted by DPPC or DPPS, when inserted into the lipid film, with different effects on the organization of these microenvironments, as a function of the lipid composition, inducing a strong disorder of the hydrophobic chains in the DPPS monolayer in contrast to the DPPC monolayer, where only the polar ester group was disturbed at lower surface pressure [58]. Furthermore, it has been shown that the activity and insertion of alkaline phosphatase is sensitive to the lateral packing and physical state of the lipid [7,28] and on defined clustering of the enzyme at the interface [59].

When comparing the kinetic parameters obtained for TNAP reconstituted into liposomes of different lipid compositions in the presence of AnxA5 for the hydrolysis of ATP (Table 2 and Fig. 3A), negative cooperativity for proteoliposomes composed only by DPPC (0.72) is observed, with a small decrease in the cooperativity values as DPPS concentration increases in the lipid bilayers (Table 2). Higher $K_{0.5}$ values were also found in the presence of

Table 2
Kinetic parameters for the substrates hydrolysis (pH 7.4) by proteoliposomes with different lipid compositions carrying TNAP alone or TNAP + AnxA5. The percentages of DPPC:DPPS are expressed in molar ratio.

Substrates	Kinetic parameters	Proteoliposomes TNAP	Proteoliposomes TNAP + AnxA5			
		DPPC	DPPC	DPPC:DPPS 5%	DPPC:DPPS 10%	DPPC:DPPS 15%
ATP	V_m (U/mg)	13.59 ± 0.67	29.85 ± 1.49	14.02 ± 0.70	15.74 ± 0.79	13.86 ± 0.69
	$K_{0.5}$ (mM)	0.068 ± 0.005	0.184 ± 0.009	0.197 ± 0.008	0.172 ± 0.009	0.279 ± 0.014
	n	1.01 ± 0.05	0.72 ± 0.03	0.63 ± 0.03	0.71 ± 0.05	0.69 ± 0.04
	$k_{cat}/K_{0.5}$ (M^{-1} s^{-1})	399.71 ± 19.98	324.46 ± 16.22	142.34 ± 7.12	183.02 ± 9.15	99.35 ± 4.97
ADP	V_m (U/mg)	5.90 ± 0.35	8.87 ± 0.53	11.56 ± 0.69	5.77 ± 0.35	4.70 ± 0.28
	$K_{0.5}$ (μM)	$1.7 \times 10^{-5} \pm 0.2 \times 10^{-5}$	60.08 ± 3.60	32.31 ± 1.94	14.87 ± 0.89	30.83 ± 1.85
	n	1.22 ± 0.05	0.71 ± 0.02	1.33 ± 0.04	1.49 ± 0.05	1.53 ± 0.05
	$k_{cat}/K_{0.5}$ (M^{-1} s^{-1})	694.12 ± 41.65	295.27 ± 17.72	715.57 ± 42.93	776.06 ± 46.56	304.90 ± 18.29
PP_i	V_m (U/mg)	17.77 ± 0.71	46.16 ± 1.85	38.13 ± 1.53	30.39 ± 1.21	24.84 ± 0.99
	$K_{0.5}$ (mM)	0.164 ± 0.007	0.131 ± 0.005	0.233 ± 0.008	0.093 ± 0.003	0.095 ± 0.005
	n	0.79 ± 0.05	0.80 ± 0.03	0.72 ± 0.03	0.85 ± 0.05	0.82 ± 0.02
	$k_{cat}/K_{0.5}$ (M^{-1} s^{-1})	216.71 ± 8.67	704.73 ± 28.19	327.30 ± 13.09	657.08 ± 26.28	524.05 ± 20.96

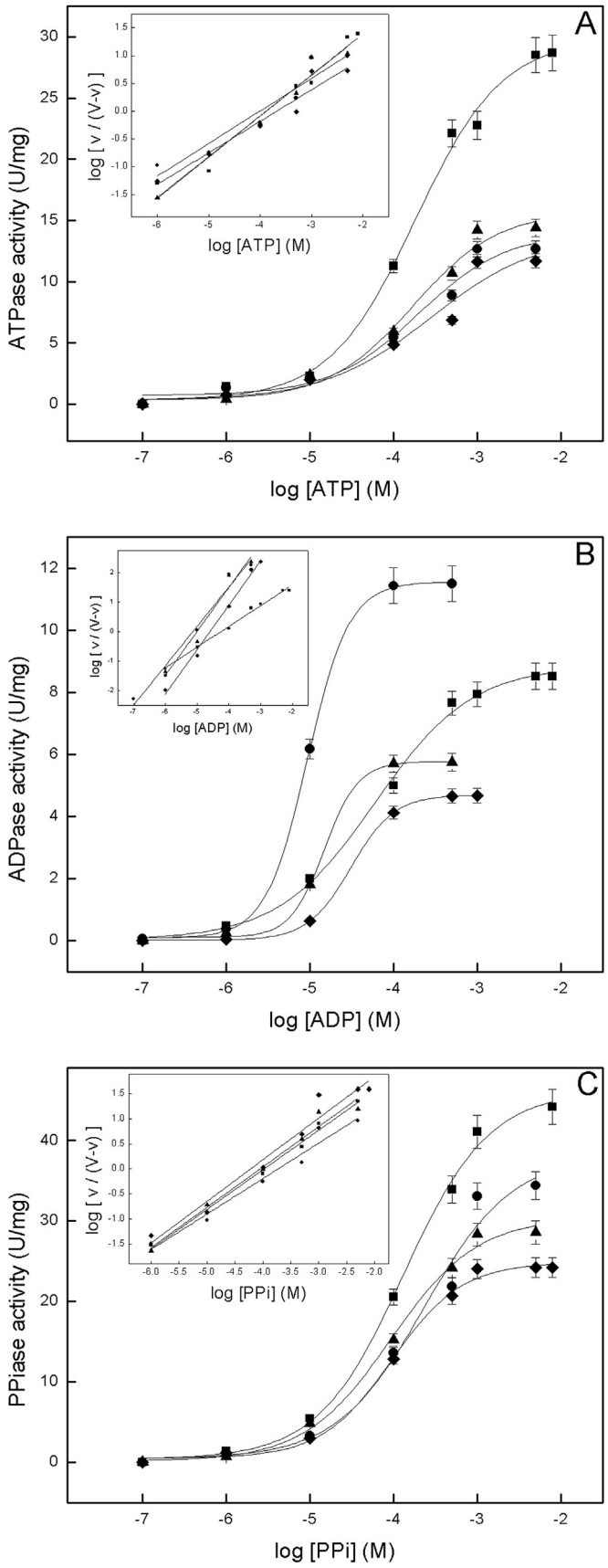

Fig. 3. Effect of the liposome composition ((■) DPPC 100%; (●) DPPC:DPPS 5%; (▲) DPPC:DPPS 10% and (◆) DPPC:DPPS 15%, molar ratio) on the kinetic parameters for substrates hydrolysis by TNAP reconstituted in proteoliposomes carrying AnxA5: (A) ATPase activity; (B) ADPase activity and (C) PP_iase activity (U/mg). Inset: Hill coefficient (n).

DPPS and AnxA5, when compared with the value obtained for DPPC-only proteoliposomes containing TNAP alone (0.068 mM) (Table 2). V_{max} values for ATP hydrolysis by TNAP decreased significantly with the presence of DPPS in the proteoliposomes (Fig. 3A) and, in the presence of AnxA5, a considerable increase in V_{max} was observed for neat DPPC-proteoliposomes (Table 2).

For ADP hydrolysis by TNAP a gradual increase in the cooperativity values was observed with the increase in the DPPS concentration in the vesicles, varying from 0.71 for DPPC-proteoliposome up to 1.53 for DPPC:DPPS 15%-proteoliposome composition (Table 2). A significant reduction in $K_{0.5}$ values was observed in the presence of DPPS when compared with DPPC proteoliposomes (Table 2). The higher V_{max} was found for the DPPC-proteoliposome containing DPPS 5% (Fig. 3B).

The presence of AnxA5 and different concentrations of DPPS in the proteoliposomes had no effect in the cooperativity values for PP_i hydrolysis by TNAP (Table 2). Higher $K_{0.5}$ value was found for the system containing DPPS 5% (Table 2) and a decrease in V_{max} was observed with increasing DPPS concentrations in the proteoliposomes (Fig. 3C). In the presence of AnxA5, a significant increase in V_{max} (more than 2-fold) was observed for DPPC proteoliposomes (Table 2).

The comparison between the catalytic efficiencies calculated for the proteoliposomes containing different DPPS concentrations (Table 2) allowed us to evaluate which DPPC:DPPS ratio was the best to reconstitute TNAP and AnxA5 concomitantly, based on the kinetic parameters obtained for the different substrates studied. For the hydrolysis of all substrates by TNAP, the best catalytic efficiency was found for DPPC:DPPS proteoliposomes containing 10% of DPPS (Table 2).

When we compared neat DPPC proteoliposomes with those containing both lipids, the best catalytic efficiency was found for proteoliposomes composed just by DPPC for the hydrolysis of PP_i by TNAP ($k_{cat}/K_{0.5} = 704.73\ M^{-1}\ s^{-1}$).

These data thus suggest that the presence of DPPS might be influencing TNAP specificity during hydrolysis of the different substrates, with a higher specificity of the enzyme for PP_i when compared with ATP and ADP, in the conditions used in this study [25,47]. As reported on previous studies, the lipid charge plays a crucial role in the interaction of proteins with lipids and can affect enzymatic activity in different ways, depending on the substrate used [47]. Moreover, the pH of the reaction medium is an important factor to be considered, once it affects significantly the hydrolysis of different substrates by TNAP [60].

3.3. Thermotropic behavior

The different liposomes and proteoliposomes samples were analyzed by DSC and the thermograms are shown in Fig. 4. The unilamellar liposomes composed of DPPC only (Fig. 4A-a) are characterized by a main phase transition temperature of 40.8 °C. Data for the main phase transition temperature (T_m), transition enthalpy (ΔH) and cooperativity of the phase transition ($\Delta t_{1/2}$) are summarized in Table 3. Similar data was obtained in previous studies [7,28,61]. The $\Delta t_{1/2}$ can be determined directly from the DSC curve since it is related to the sharpness of the transition peak, which is given by the temperature width at half-height of the DSC trace [62]. With 10% of DPPS in the DPPC membrane, there is a broadening of the transition peaks due to a decrease of the phase transition cooperativity and ΔH values (Table 3 and Fig. 4A-b). Therefore, the gel–fluid transition process is less cooperative when the DPPS is present in the membrane. Is known that the presence of impurities or others compounds within the bilayers broadens the transition peak. Thus, for complex lipid mixtures $\Delta T_{1/2}$ reaches values of 10–15 °C [63–65].

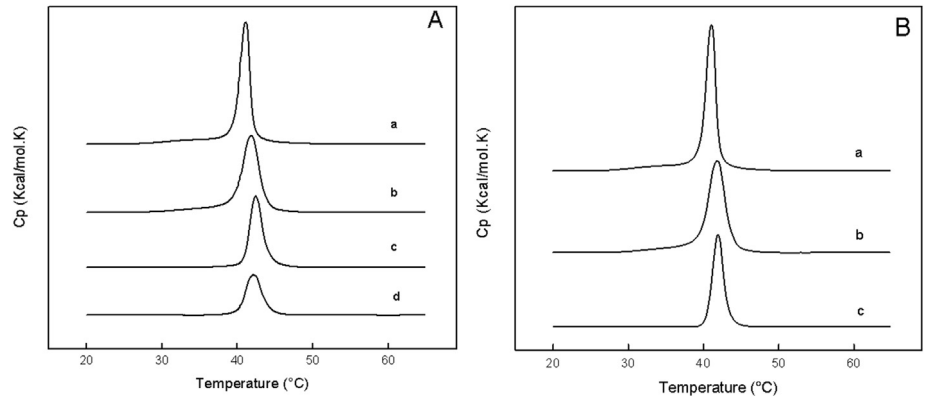

Fig. 4. DSC thermograms of liposomes and proteoliposomes. (A) DSC thermograms were registered using a Nano-DSC II calorimeter and processed in Excess heat capacity, Cp (kcal/K mol), as a function of temperature (°C) for vesicles constituted by DPPC and DPPC:DPPS 10% (molar ratio) containing TNAP and AnxA5: [a] DPPC-liposomes; [b] DPPC:DPPS 10%-liposomes; [c] DPPC:DPPS 10%-proteoliposomes containing TNAP + AnxA5 and [d] DPPC:DPPS 10%-proteoliposomes containing TNAP. (B): [a] DPPC-liposomes; [b] DPPC:DPPS 10%-liposomes and [c] DPPC:DPPS 10%-proteoliposomes containing AnxA5.

The average diameters of the DPPC:DPPS liposomes did not vary significantly when compared with the diameter obtained for DPPC-vesicles and low polydispersity index (PI) values were obtained for the different liposomes, indicating that the samples were nearly monodisperse in size (Table 3). The stability of the different vesicular systems (liposomes and proteoliposomes) was also evaluated by DLS by monitoring both the diameter and intensity throughout the period of use of the samples. The sizes of the vesicles were uniform for ~7 days and varied less than 5% (data not shown).

The thermotropic behavior of TNAP-proteoliposomes and AnxA5-proteolipomes are also shown in Fig. 4 where one can observe that the presence of AnxA5 causes a decrease in ΔH values as compared with the respective liposomes systems (Table 3 and Fig. 4B). When TNAP is present on the proteoliposomes, these effects are even greater besides a broadening of the transition peaks (Table 3 and Fig. 4A). Similar data were reported before by our research group [7,28], so we conclude that the strong decrease observed for ΔH value of TNAP-proteoliposomes when compared to liposomes was related mainly to the GPI anchor insertion. According to Papahadjopoulos [66], the binding way of the lipid–protein interaction can be determined from the effect of the protein on the gel-to-liquid crystalline lipid phase transition. In fact, the binding of a peripheral membrane protein to the bilayer surface is followed by the partial insertion of the protein into the bilayer, where it interacts with the lipid hydrocarbon chains, a decrease in Tm and/or ΔH is observed, which might be explained by a decrease of van der Waals interactions between lipid acyl chains after protein insertion [62]. In the case of TNAP, the insertion of the anchor into membrane surface leads to a decrease in T_m and/or ΔH, which might be explained by a decrease of van der Waals interactions between lipid acyl chains after GPI anchor insertion [7]. These proteins are believed to interact with phospholipid bilayers driven by a combination of electrostatic and hydrophobic forces [62]. Generally, peripheral proteins initially adsorb to the charged polar head groups of the phospholipids and subsequently partially penetrate the hydrophilic–hydrophobic interface of the bilayer to interact with a portion of the lipid hydrocarbon chains. These proteins normally raise phospholipid monolayers and alter the permeability of phospholipid vesicles into which they are incorporated [62].

On the other hand, amphitropic proteins, such as the Annexins [67–69], can deeply penetrate into the hydrophobic core of the lipid bilayers and prevent some lipid molecules from participating in the melting transition. As a consequence, these proteins have little effect on T_m promoting a linear decrease of ΔH, with increasing protein concentration [62]. The interaction of AnxA5 with the DPPC and DPPC:DPPS 10% liposomes also is manifested through a decrease of the $\Delta t_{1/2}$ values. Furthermore, when TNAP interacts with these liposomes there is an increase of the $\Delta t_{1/2}$ values.

An interesting effect is observed when AnxA5 is present in the TNAP-proteoliposomes constituted of DPPC and DPPC:DPPS 10% (molar ratio). When only TNAP is reconstituted in DPPC-liposomes, we obtain around 41% of the reconstituted activity (Table 1) and observe an intense decrease in the transition phase enthalpy (3.58 kcal mol^{-1}) as compared to the respective liposome

Table 3
Biophysical and biochemical characterization of liposomes and proteoliposomes constituted by DPPC and DPPC:DPPS 10% (molar ratio) harboring TNAP, AnxA5 and TNAP + AnxA5. DSC thermodynamic parameters and DLS values.

Liposome/proteoliposome composition			Diameter (nm)	PI	ΔH_{total} (Kcal mol^{-1})	T_m (°C)	$\Delta t_{1/2}$
Lipid (molar ratio)	TNAP	AnxA5					
*DPPC 100%	–	–	143.2 ± 3.03	0.102 ± 0.04	8.73 ± 0.05	40.8 ± 0.01	1.29 ± 0.01
*DPPC:DPPS 10%	–	–	131.8 ± 0.47	0.057 ± 0.02	8.43 ± 0.07	41.9 ± 0.02	1.96 ± 0.02
**DPPC 100%	+	–	226.5 ± 4.36	0.426 ± 0.05	3.58 ± 0.02	40.9 ± 0.01	1.32 ± 0.01
**DPPC 100%	–	+	271.8 ± 9.87	0.385 ± 0.18	5.68 ± 0.05	41.0 ± 0.01	0.96 ± 0.01
**DPPC 100%	+	+	270.0 ± 8.01	0.465 ± 0.03	6.38 ± 0.05	41.4 ± 0.01	1.16 ± 0.01
**DPPC:DPPS 10%	+	–	206.5 ± 8.91	0.372 ± 0.25	4.34 ± 0.02	42.2 ± 0.02	2.19 ± 0.01
**DPPC:DPPS 10%	–	+	221.5 ± 8.30	0.360 ± 0.02	5.37 ± 0.02	42.0 ± 0.01	1.50 ± 0.01
**DPPC:DPPS 10%	+	+	248.1 ± 8.98	0.476 ± 0.08	5.56 ± 0.04	42.4 ± 0.02	1.76 ± 0.01

*Liposomes.
**Proteoliposomes.

(8.73 kcal mol^{-1}) (Table 3). However, when AnxA5 is introduced in that lipid system, it promotes an increase in the reconstituted TNAP activity (64%, Table 1) and also a significant increase in the enthalpy of the system (6.38 kcal mol^{-1}). Similar behavior can be observed for DPPC:DPPS 10%-proteoliposomes (Tables 1 and 3).

Low values of TNAP's activity incorporated into DPPC-liposomes were obtained when compared with our previous data [7,26,28], probably due to presence of EGTA in the reaction medium, which is necessary for the calcium uptake by AnxA5. Besides Ca^{2+} ions, EGTA may be chelating Mg^{2+} ions also, which are essential for TNAP's activity, thus decreasing the reconstituted enzyme's activity.

The presence of both proteins, together or separately, does not affect significantly the T_m, when compared with the respective liposome composition (Table 3).

The presence of transmembrane protein (AnxA5) significantly changes the thermodynamic parameters of the lipid membranes (Table 3) resulting in the different lipid packing around anchored protein (TNAP). This event probably causes the changes in kinetic behavior (Table 2) of TNAP, as observed in the 3.2 item. Such an effect was observed previously using *in situ* p-polarized light Fourier transform-infrared reflection–absorption spectroscopic (FT-IRRAS) measurements [70]. The authors showed the formation of monolayers interacting with TNAP without appreciable loss of its conformation/orientation at the air–water interface even at high surface pressures. This effect can be attributed to the presence of hydrophobic anchor that drives the enzyme stability at the air–water interface conferring a minimum adsorption free energy with no need for internal hydrophobic group exposure. The presence of a model lipid at the interface regulates the arrangement of the enzyme at the monolayer, orienting the α-helix main axis in a suitable position. Furthermore, the positioning of the GPI anchor and lipid hydrophobic chains can be varied with increasing surface pressures [70]. Thus, the presence of different lipids and its biophysical properties are key factors that can control the orientation of the enzyme when incorporating in model membranes as well as they can modulate the kinetic behavior. In terms of MVs, our results point to the special interplay between lipid composition and the function of the proteins (AnxA5 and TNAP) responsible for the biological process of biomineralization.

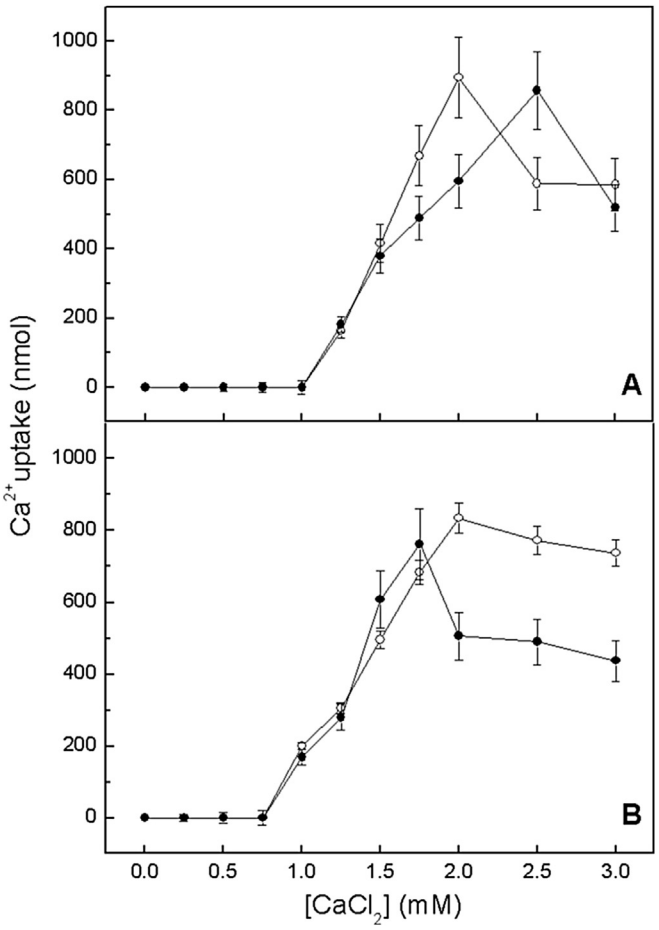

Fig. 5. Ca^{2+} influx into the proteoliposomes of different lipid compositions (○) DPPC-proteoliposomes and (●) DPPC:DPPS 10%-proteoliposomes: (A) Proteoliposomes carrying AnxA5 and (B) Proteoliposomes carrying AnxA5 and TNAP. The background values of liposomes were discounted from the values obtained for the respective proteoliposomes.

3.4. Ca^{2+} influx into the proteoliposomes

In order to evaluate whether AnxA5 is functional upon incorporation into the proteoliposomes, Ca^{2+} influx into the proteoliposomes containing DPPC and DPPC:DPPS 10% (molar ratio) was measured. The proteoliposomes were incubated with a fixed concentration of $^{45}Ca^{2+}$ (5.5 μCi mL^{-1}) and increasing concentrations of cold Ca^{2+} (from 0.5 to 5 mM), resulting in a linear increased uptake, reaching a maximum value with 2 mM Ca^{2+} in the DPPC system, and 2.5 mM in the DPPC:DPPS system (Fig. 5A). Thus, around 600 nmol Ca^{2+}/mg of total lipid were incorporated into the vesicles (Fig. 5). Liposomes constituted by DPPC and DPPC:DPPS 10% were used as controls of vesicles without proteins (background). The values of unspecific interaction between $^{45}Ca^{2+}$ and the membrane of liposomes were discounted from the values obtained for the respective proteoliposomes.

Although the levels of Ca^{2+} vary from cell to cell, generally it is accepted that Ca^{2+} concentrations in extracellular physiologic fluids are around 2 mM and there is a significant difference when compared to the intracellular concentrations (around 10 μM) [71]. Mean values of cytosolic Ca^{2+} in cells from the various zones of the growth plate are quite similar, but levels in individual cells and subcellular compartments vary significantly [72].

DPPS lipid has a negative charge and attracts by electrostatic affinity the Ca^{2+} ions in the external surface of the vesicles, probably resulting in a smaller number of ions available in solution to be transported to inside the proteoliposomes. Thus, a large Ca^{2+} concentration is needed in the reaction medium (2.5 mM) in order to obtain a similar uptake when compared with proteoliposomes in the DPPS absence (2 mM). In addition, EGTA was used to control the calcium concentration in the buffer. For this reason, EGTA can chelate calcium, decreasing its free concentration in the solution and thus providing less free ions to be transported into the proteoliposomes.

When interpreting the values of the scintillation counting obtained for the liposomes samples used as controls for the respective proteoliposomes, we observed that in the DPPS presence the baseline values were always greater, reinforcing the hypothesis of the surface interaction between Ca^{2+} and DPPS [1,9,12].

However, the behavior of both proteoliposomes is very similar and after saturation a decrease of the Ca-uptake was observed. The presence of TNAP in the proteoliposomes (Fig. 5B) did not affect significantly AnxA5-mediated Ca^{+2} transports. On the other hand, the presence of AnxA5 affected significantly the hydrolysis of PP_i, ATP and ADP by TNAP, as seen in the previous section.

3.5. Effect of AnxA5 presence on giant lipid vesicles behavior

In order to investigate whether the insertion of AnxA5 into proteoliposomes affects the membrane permeability to ions such as

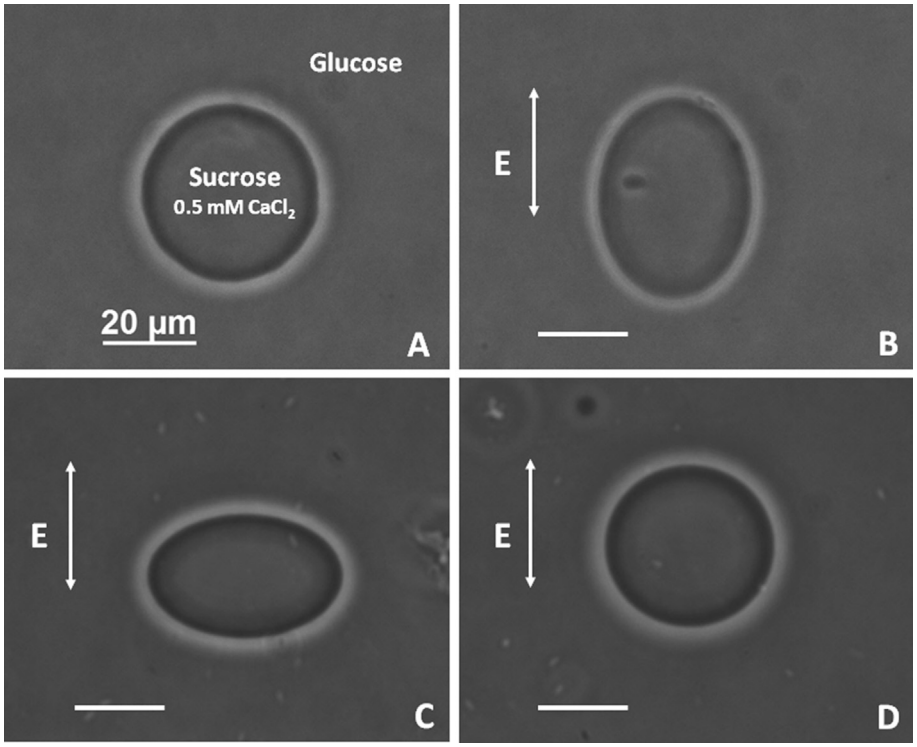

Fig. 6. Morphological changes of GUVs exposed to an electric field (10 V, 1 MHz) in the presence or absence of the AnxA5. Images obtained in phase contrast, objective 60x and scale bar corresponds to 20 μm. (A) GUVs constituted by DOPC with 0.5 mM $CaCl_2$ in the inner compartment exhibit spherical shape; (B) Under the electric field the GUVs assume prolate shapes; (C) GUVs incubated with AnxA5 (8.22 μM) and subjected to the electrical field display oblate shapes; (D) GUVs recovered its initial spherical shape with time (~20 min) after the outer and inner solution conductivities are equilibrated.

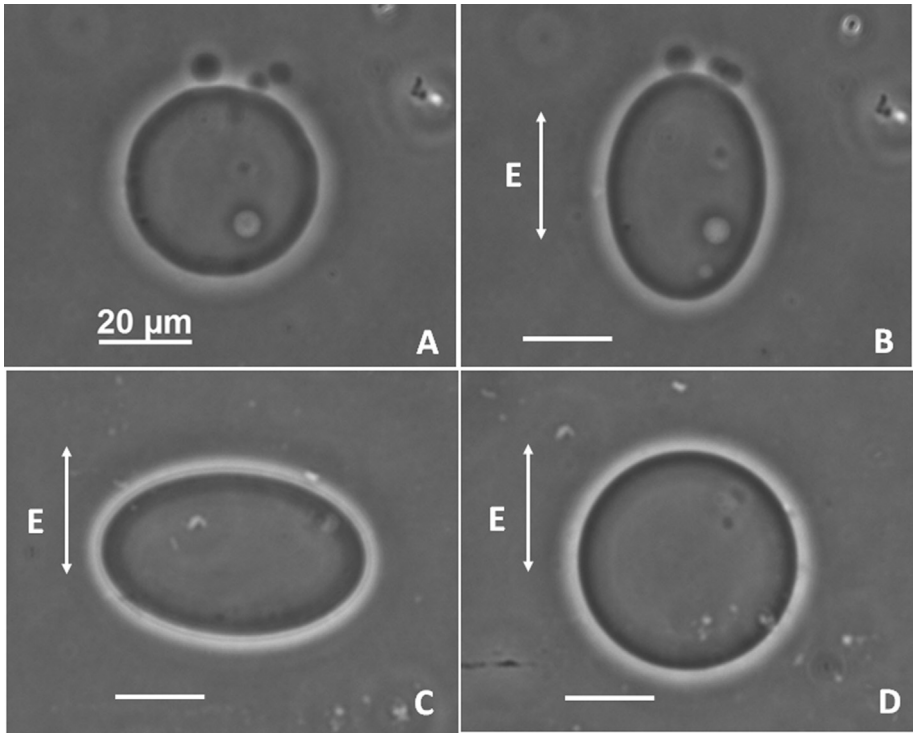

Fig. 7. Morphological changes of GUVs exposed to an electric field (10 V, 1 MHz) in the presence or absence of the AnxA5. Images obtained in phase contrast, objective 60x and scale bar corresponds to 20 μm. (A) GUVs constituted by DOPC:DPPS 10% (molar ratio) with 0.5 mM $CaCl_2$ in the inner compartment exhibit spherical shape; (B) Under the electric field the GUVs assume prolate shapes; (C) GUVs incubated with AnxA5 (8.22 μM) and subjected to the electrical field display oblate shapes; (D) GUVs recovered its initial spherical shape with time (~20 min) after the outer and inner solution conductivities are equilibrated.

Ca^{2+}-transport, model membranes represented by giant unilamellar vesicles, GUVs, were thereby considered. GUVs constituted by DOPC and DOPC:DPPS 10% (molar ratio) were grown containing 0.5 mM $CaCl_2$ in the inner compartment and dispersed in the salt-free outer solution. In this way, the conductivity of the inner solution was initially higher in respect to the outer solution.

AnxA5-free unilamellar vesicles initially spherical (Fig. 6A) present a morphological transition to a prolate-like shape (Fig. 6B) under an electric field, thus exposing the hidden surface area due to thermal fluctuations [52]. On the other hand, vesicles dispersed in AnxA5-containing glucose solution under the AC electric field exhibited initially oblate shape (Fig. 6C), without loss of vesicle optical contrast that would characterize pores opening [52]. Such an observation demonstrates that the protein-membrane interaction impacts on the GUVs morphology. In the time sequence, the GUV spherical shape is thus recovered (Fig. 6D). This finding must be due to the salt release from the inner to the outer GUV solution, thus equilibrating the internal and external conductivities [54]. The same behavior is observed in vesicles constituted by DOPC:DPPS 10% (molar ratio) (Fig. 7). These results confirm the functional AnxA5 insertion into the different membrane mimetic systems studied, showing its Ca^{2+}-transport role in both systems constituted by DOPC and DOPC:DPPS 10%. Future experiments will address how AnxA5 forms the channel and how calcium ions are transported [9].

4. Conclusions

A fundamental understanding of the interplay between lipid compositions and membranes behavior is crucial for the validation of these systems as mimetic of the process of biomineralization. MVs comprise complex systems with various ionic channels and transporters, containing a group of enzymes responsible for controlling the P_i/PP_i ratio in the extracellular medium. Therefore, it is very important to employ proteoliposomes as membrane mimetic systems in order to understand how the presence of different combined proteins affects their functions in the membrane. Here we report stable systems of proteoliposomes harboring TNAP and AnxA5, followed by their characterization. These promising mimetic systems successfully transport Ca^{2+} into the vesicles and possess an enzyme able to hydrolyze phosphosubstrates in the lipid–water interface. The presence of TNAP in the proteoliposomes did not significantly affect AnxA5-mediated Ca^{+2} transports. On the other hand, one can observe that the presence of AnxA5 affects significantly the hydrolysis of substrates by TNAP.

Admittedly, this proteoliposome system is still incomplete since other proteins are necessary to adequately mimic the MVs in the biomineralization process, such as the protein Pit-1 for example, which may be responsible for the P_i influx into the vesicles. However, in order to obtain proteoliposomes containing three proteins simultaneously (e.g. TNAP, AnxA5 and Pit-1), a systematic study regarding the functional incorporation of each protein in succession is necessary in addition to a determination of the appropriate lipid composition, thus gradually increasing the complexity of the biomimetic system. Certainly, the presence of one protein may cause significant changes in the behavior of the other incorporated proteins as we show here for AnxA5 and TNAP. Taken together, these results will be of great help to better understand the complex mechanisms involved in the interaction of a specific protein with the lipid bilayer components enrolled in the biomineralization process.

Acknowledgments

The authors thank Dr. Omar Mertins for helpful assistance in GUVs experiments, Prof. Dr. Bruno Maggio for assistance in DSC analysis and Priscila Cerviglieri for linguistic advice. This work was supported in part by grants DE12889 and AR53102 from the National Institutes of Health, USA. We also thank FAPESP (2014/11941-3), CAPES (NanoBiotech) and CNPq (400146/2014-2 and 443758/2014-0). for the financial support given to our laboratory. MB and AMSS received a CAPES and FAPESP scholarship, respectively. PC and RI also acknowledge CNPq for research fellowships.

References

[1] R.E. Wuthier, Fed. Proc. 35 (1976) 117–121.
[2] H.C. Anderson, Scan. Electron. Microsc. Pt. 2 (1984) 953–964.
[3] H.C. Anderson, Curr. Rheumatol. Rep. 5 (2003) 222–226.
[4] C. Thouverey, A. Strzelecka-Kiliszek, M. Balcerzak, R. Buchet, S.J. Pikula, Cel. Biochem. 106 (2009) 127–138.
[5] R. Buchet, S. Pikula, D. Magne, S. Mebarek, Methods Mol. Biol. 1053 (2013) 115–124.
[6] D. Abdallah, E. Hamade, R.A. Merhi, B. Bassam, R. Buchet, S. Mebarek, Biochem. Biophys. Res. Commun. 446 (4) (2014) 1161–1164, 18.
[7] M. Bolean, A.M.S. Simão, B.Z. Favarin, J.L. Millán, P. Ciancaglini, Biophys. Chem. 152 (2010) 74–79.
[8] M. Balcerzak, E. Hamade, L. Zhang, S. Pikula, G. Azzar, J. Radisson, J. Bandorowicz-Pikula, R. Buchet, Acta Biochim. Pol. 50 (2003) 1019–1038.
[9] R.E. Wuthier, G.F. Lipscomb, Front. Biosci. 17 (2011) 2812–2902.
[10] E.E. Golub, Semin. Immunopathol. 5 (2011) 409–417.
[11] T. Kirsch, Connect. Tissue Res. 6 (2012) 438–445.
[12] T. Kirsch, Front. Biosci. 10 (2005) 576–581.
[13] R. Huber, J. Romisch, E.P. Pâques, EMBO J. 9 (1990) 3867–3874.
[14] S. Liemann, R. Huber, Cell Mol. Life Sci. 53 (1997) 516–521.
[15] T. Kirsch, H.D. Nah, D.R. Demuth, G. Harrison, E.E. Golub, S.L. Adams, M. Pacifici, Biochem. 36 (1997) 3359–3367.
[16] R. Hauptmann, I. Maurer-Fogy, E. Krystek, G. Bodo, H. Andree, C.P.M. Reutelingsperger, Eur. J. Biochem. 185 (1989) 63–71.
[17] H.A.M. Andree, M.C.A. Stuart, W.T. Hermens, C.P.M. Reutelingsperger, H.C. Hemker, P.M. Frederik, G.M. Willems, J. Biol. Chem. 267 (1992) 17907–17912.
[18] D.D. Schlaepfer, H. Jones, H.T. Haigler, Biochem. 31 (1992) 1886–1891.
[19] F.F. Davidson, M.D. Lister, E.A. Dennis, J. Biol. Chem. 265 (1990) 5602–5609.
[20] P. Ciancaglini, M.C. Yadav, A.M.S. Simão, S. Narisawa, J.M. Pizauro, C. Farquharson, M.F. Hoylaerts, J.L. Millán, J. Bone Min. Res. 25 (2010) 716–723.
[21] M.C. Yadav, A.M.S. Simão, S. Narisawa, C. Huesa, M.D. McKee, C. Farquharson, J.L. Millán, J. Bone Min. Res. 26 (2011) 286–297.
[22] F.A. Leone, J.M. Pizauro, P. Ciancaglini, Trends Comp. Biochem. Physiol. 3 (1997) 57–73.
[23] J.M. Pizauro, P. Ciancaglini, F.A. Leone, Mol. Cel. Biochem. 152 (1995) 121–129.
[24] A.M.S. Simão, M.M. Beloti, A.L. Rosa, P.T. de Oliveira, J.M. Granjeiro, J.M. Pizauro, P. Ciancaglini, Cell Biol. Int. 31 (2007) 1405–1413.
[25] P. Ciancaglini, A.M.S. Simão, M. Bolean, J.L. Millán, C.F. Rigos, J.S. Yoneda, M.C. Colhone, R.G. Stabeli, Biophys. Rev. 4 (2012) 67–81.
[26] F.L. Camolezi, K.P.R. Daghastanli, P.P. Magalhães, J.M. Pizauro, P. Ciancaglini, Int. J. Biochem. Cell Biol. 34 (2002) 1091–1101.
[27] D.F. Ierardi, J.M. Pizauro, P. Ciancaglini, Biochim. Biophys. Acta 1567 (2002) 183–192.
[28] M. Bolean, A.M.S. Simão, B.Z. Favarin, J.L. Millán, P. Ciancaglini, Biophys. Chem. 158 (2011) 111–118.
[29] M.C. Giocondi, F. Besson, P. Dosset, P.E. Milhiet, C. Le Grimellec, Langmuir 23 (2007) 9358–9364.
[30] J.L. Millán, Wiley-VCH Verlag GmbH & Co. KGaA, Weinheim, 2006.
[31] J.M. Pizauro, P. Ciancaglini, F.A. Leone, Biochim. Biophys. Acta 1202 (1993) 22–28.
[32] J.M. Pizauro, C. Curti, P. Ciancaglini, F.A. Leone, Comp. Biochem. Physiol. 87B (1987) 921–926.
[33] L. Zhang, M. Balcerzak, J. Radisson, C. Thouverey, S. Pikula, G. Azzar, R. Buchet, J. Biol. Chem. 280 (2005) 37289–37296.
[34] A.A. Rezende, J.M. Pizauro, P. Ciancaglini, F.A. Leone, Cel. Mol. Biol. 44 (1998) 293–302.
[35] J.L. Millán, Purinergic. Signal 2 (2006) 335–341.
[36] A.M.S. Simão, M.C. Yadav, P. Ciancaglini, J.L. Millán, Braz. J. Med. Biol. Res. 43 (2010) 234–241.
[37] B.D. Boyan, Z. Schwartz, L.D. Swain, A. Khare, Anat. Rec. 224 (1989) 211–219.
[38] E.D. Eanes, A.W. Hailer, Calcif. Tissue Int. 37 (1985) 390–394.
[39] L.N.Y. Wu, B.R. Genge, D.G. Dunkelberger, R.Z. LeGeros, B. Concannon, R.E. Wuthier, J. Biol. Chem. 272 (1997) 4404–4411.
[40] L.N.Y. Wu, B.R. Genge, M.W. Kang, A.L. Arsenault, R.E. Wuthier, J. Biol. Chem. 277 (2002) 5126–5133.
[41] M. Damek-Poprawa, E.E. Golub, L. Otis, G. Harrison, C. Phillips, Biochem. 45 (2006) 3325–3336.
[42] S.E. Logue, M. Elgendy, S.J. Martin, Nat. Protoc. 4 (2009) 1383–1395.

[43] A.M.S. Simão, M.M. Beloti, R.M. Cezarino, A.L. Rosa, J.M. Pizauro, P. Ciancaglini, Comp. Biochem. Physiol. A Mol. Integr. Physiol. 146 (2007) 679–687.
[44] E.F. Hartree, Anal. Biochem. 48 (1972) 422–427.
[45] F.A. Leone, J.A. Baranauskas, R.P. Furriel, I.A. Borin, Biochem. Mol. Biol. Educ. 33 (2005) 399–403.
[46] P. Ciancaglini, A.M.S. Simão, F.L. Camolezi, J.L. Millán, J.M. Pizauro, Braz. J. Med. Biol. Res. 39 (2006) 603–610.
[47] A.M.S. Simão, M.C. Yadav, S. Narisawa, M. Bolean, J.M. Pizauro, M.F. Hoylaerts, P. Ciancaglini, J.L. Millán, J. Biol. Chem. 285 (2010) 7598–7609.
[48] H. de Lima Santos, M.L. Lopes, B. Maggio, P. Ciancaglini, Coll. Surf. B Biointerf. 41 (2005) 239–248.
[49] G.A. dos Santos, C.H. Thomé, G.A. Ferreira, J.S. Yoneda, T.M. Nobre, K.R. Daghastanli, P.S. Scheucher, H.L. Gimenes-Teixeira, M.G. Constantino, K.T. de Oliveira, V.M. Faça, R.P. Falcão, L.J. Greene, E.M. Rego, P. Ciancaglini, Biochim. Biophys. Acta 1798 (2010) 1714–1723.
[50] H.H.T. Hsu, N.P. Camacho, Atherosclerosis 143 (1999) 353–362.
[51] M.I. Angelova, D.S. Dimitrov, Faraday Discuss. 81 (1986) 303–311.
[52] O. Mertins, I.O.L. Bacellar, F. Thalmann, C.M. Marques, M.S. Baptista, R. Itri, Biophys. J. 106 (2014) 162–171.
[53] K.A. Riske, R. Dimova, Biophys. J. 88 (2005) 1143–1155.
[54] S. Aranda, K.A. Riske, R. Lipowsky, R. Dimova, Biophys. J. 95 (2008) L19–L21.
[55] S. Sesana, F. Re, A. Bulbarelli, D. Salerno, E. Cazzaniga, M. Masserini, Biochem. 47 (2008) 5433–5440.
[56] C. Liu, P. Marshall, I. Schreibman, A. Vu, W. Gai, M. Whitlow, Blood 93 (1999) 2297–2301.
[57] E. Bellet-Amalric, D. Blaudez, B. Desbat, F. Graner, F. Gauthier, A. Renault, Biochim. Biophys. Acta 1467 (2000) 131–143.
[58] F. Ronzon, B. Desbat, J.P. Chauvet, B. Roux, Biochim. Biophys. Acta 1560 (2002) 1–13.
[59] L. Caseli, R.G. Oliveira, D.C. Masui, R.P. Furriel, F.A. Leone, B. Maggio, M.E. Zaniquelli, Langmuir 21 (2005) 4090–4095.
[60] A.M.S. Simão, M. Bolean, M.F. Hoylaerts, J.L. Millán, P. Ciancaglini, Calcif. Tissue Int. 93 (2013) 222–232.
[61] T.B. Pedersen, M.C. Sabra, S. Frokjaer, O.G. Mouritsen, K. Jørgensen, Chem. Phys. Lipids 113 (2001) 83–95.
[62] J.H. Kleinschmidt, Lipid-protein interactions: methods and protocols, ISBN: 978-1-62703-274-2, in: H. Jörg (Ed.), Kleinschmidt, Humana Press., Kassel, Germany, 2013.
[63] R.N. McElhaney, Chem. Phys. Lipids 30 (1982) 229–259.
[64] R.N. McElhaney, Biochim. Biophys. Acta 864 (1986) 361–421.
[65] C. Demetzos, J. Liposome Res. 18 (2008) 159–173.
[66] D. Papahadjopoulos, M. Moscarello, E.H. Eylar, T. Isac, Biochim. Biophys. Acta 401 (1975) 317–335.
[67] T.C. Yen, S.P. Wey, C.H. Liao, C.H. Yeh, D.W. Shen, S. Achilefu, T.C. Wun, Anal. Biochem. 406 (2010) 70–79.
[68] F. Wu, A. Gericke, C.R. Flach, T.R. Mealy, B.A. Seaton, R. Mendelsohn, Biophys. J. 74 (1998) 3273–3281.
[69] Z. Chen, Y. Mao, J. Yang, T. Zhang, L. Zhao, K. Yu, M. Zheng, H. Jiang, H. Yang, Proteins 82 (2014) 312–322.
[70] L. Caseli, D.C. Masui, R.P. Furriel, F.A. Leone, M.E. Zaniquelli, J. Orbulescu, R.M. Leblanc, J. Colloid Interface Sci. 320 (2) (2008) 476–482, 15.
[71] A.C. Tas, Acta Biomater. 10 (2014) 1771–1792.
[72] L.N. Wu, M.G. Wuthier, B.R. Genge, R.E. Wuthier, Clin. Orthop. Relat. Res. 335 (1997) 310–324.